J|A|C|S COMMUNICATIONS

Published on Web 01/20/2009

Organization of Nanoparticles in Polymer Brushes

Ron Oren,[†] Ziqi Liang,[†] Jonathan S. Barnard,[‡] Scott C. Warren,[§] Ulrich Wiesner,[§] and Wilhelm T. S. Huck*,[†]

Melville Laboratory for Polymer Synthesis, Department of Chemistry, University of Cambridge, Lensfield Road, Cambridge, U.K., Department of Materials Science and Metallurgy, University of Cambridge, Pembroke Street, Cambridge, U.K., and Department of Materials Science and Engineering, Cornell University, Ithaca, New York 14853-1501

Received November 17, 2008; E-mail: wtsh2@cam.ac.uk

The mixing of nanoparticles (NPs) and polymers offers synthetic routes to nanostructured materials and composites that can be used in a wide range of applications ranging from energy generation and storage to plasmonics to ultrastrong nanocomposites.[1,2] Recent studies on nanoparticles with specially tailored surface properties and their interactions with microphase-separating block copolymers have highlighted the importance of both entropic and enthalpic driving forces for the formation of hierarchically structured materials.[3−10] The balance of interactions between hard particles and polymer chains leads to spatially periodic self-assembled structures, where particles are either excluded or incorporated in the block copolymer domains.[7,10] For example, Warren et al. showed that small silica NPs are incorporated into the PEO-domain of poly(isoprene-*b*-ethylene oxide) (PI-*b*-PEO), while NPs that are larger than the PEO end-to-end distance segregate out.[4] This self-organization can be rationalized by considering the interplay of favorable interactions between the NPs and PEO and entropy loss of the chains wrapping the NPs. Kramer and co-workers have directed NPs into either domain or the interface of a poly(2-vinylpyridine-*b*-styrene) (P2VP-*b*-PS) matrix by changing the ratio of PS to P2VP ligands on the NPs[8] or the areal density of PS ligands,[9] and relying on the strong interaction between gold and PVP.[11]

We have recently reported the formation of hybrid photovoltaic devices based on polymer brushes infiltrated with NPs.[12] Although device performance had clearly improved due to NPs infiltrating the brushes, the conditions that govern infiltration are unknown. Recent theoretical work has modeled nanoparticles entering polymer brushes.[13−15] For particles that are miscible with the polymer, the particles will infiltrate the brush to the depth where particle size and local polymer coil size (i.e., "blob" size)[13] are equal. It is expected that the extent of infiltration depends on the physical characteristics of the brushes only.

Several groups have investigated the formation of NPs inside polymer brushes[16] or on top of brushes.[17,18] However, few experimental studies of NP infiltration into polymer brushes exist. Bhat and Genzer[19] followed the uptake of Au NPs by hydrophilic brushes using UV−vis absorption and reported 3.5 nm particles infiltrating the brush only when the grafting density (σ) was low; 16 nm particles, on the other hand, remained on top of the brush at every grafting density.

Here we report the first direct visualization of polymer-coated Au NPs infiltrated into poly(4-vinylpyridine-*b*-styrene) (P4VP-*b*-PS) block copolymer brushes using cross-sectional TEM. Our experimental procedure is outlined in Scheme 1. TEMPO-terminated monolayers were prepared from tertiary bromide silanes using a modified literature procedure (see Supporting Information (SI)).[20,21] XPS data showed the disappearance of the Br 3d signal at 71 eV and the appearance of the TEMPO N 1s at 400 eV (Figure S2). P4VP brushes were grown from a 4-vinylpyridine (4VP)/toluene solution (3:1), in the presence of sacrificial initiator (0.05% to 4VP), at 130 °C for 3 h to yield 21 nm thick P4VP layers. PS brushes were grown in an identical fashion on P4VP-modified substrates to yield a 37 nm total film thickness (16 nm PS). PS brushes were also grown on control surfaces (initiator monolayer only). By comparing the molecular weight from PS formed in solution and the brush thickness, we were able to determine the grafting density of the PS blocks in the range of $\sigma_{PS} \approx 0.2$ chains nm^{-2} (see SI).

Scheme 1. Schematic Illustration of Au NP Infiltration into Block Copolymer Brushes

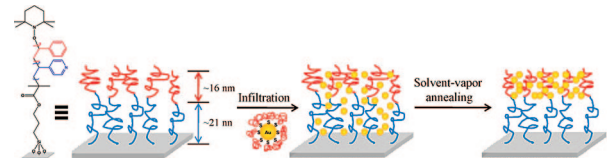

PS-covered Au NPs (2.2 nm) with surface coverage (Σ_{PS}) varying from 0.95 to 1.79 chains nm^{-2} were synthesized following literature procedures.[9] For infiltration, brushes were immersed in a 1 mg mL^{-1} solution of Au NPs in $CHCl_3$ for 1 day.

Cross-sectional samples were made using the small angle cleavage technique,[22] which is an effective method of producing ultrathin films without introducing artifacts. The thickness of the samples in the areas that are imaged in the figures below was in the range 80−100 nm as determined two-beam electron diffraction (see SI).[23]

Scanning transmission electron microscopy images were recorded in either bright-field (BF-STEM) or high annular angle dark field (HAADF-STEM) mode; the intensity was inverted on the HAADF-STEM for improved visibility.

The STEM images clearly establish that the Au NPs are separated from each other and have a core size of ∼2.2 nm with a standard deviation of ∼15%, in excellent agreement with STEM images of the particles directly after synthesis (Figure S3). An energy dispersive X-ray (EDX) spectrum verifies the presence of the Au (Figure S4).

BF-STEM images of P4VP-*b*-PS copolymer brushes infiltrated with PS-covered Au NPs are shown in Figures 1 and S4b, indicating that gold colloids are randomly dispersed throughout the PS and P4VP blocks without noticeable signs of aggregation. The film thickness in Figure 1 is ∼40 nm, in good agreement with the original ellipsometric film thickness.

[†] Department of Chemistry, University of Cambridge.
[‡] Department of Materials Science and Metallurgy, University of Cambridge.
[§] Cornell University.

10.1021/ja8090092 CCC: $40.75

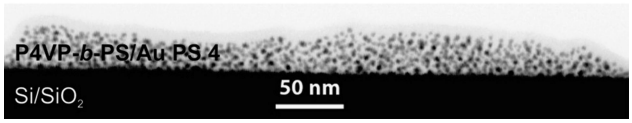

Figure 1. Cross-sectional BF-STEM images of a P4VP-*b*-PS brush (21 + 16 nm) infiltrated with PS-covered Au NP.

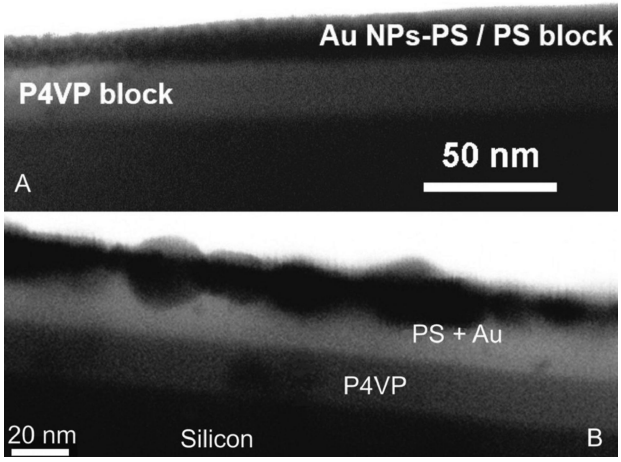

Figure 2. Cross-sectional HAADF-STEM images of P4VP-*b*-PS brushes infiltrated with PS-covered Au NP after annealing with CH_2Cl_2 vapor: (a) $\Sigma_{PS} = 1.79$ chains nm^{-2} and (b) $\Sigma_{PS} = 0.95$ chains nm^{-2}. The intensity of the images was inverted for improved visibility. The gradient in brightness, most noticeable in (a), arises from the variation in sample thickness, due to sample preparation. Layer thicknesses of 16 nm P4VP and 20 nm PS in Figure 2b are in good agreement with original layer thicknesses of 13 and 19 nm, respectively.

The presence of particles in the P4VP-layer is surprising, as the PS-coating should favor phase separation from this block, and we hypothesize that this structure is kinetically trapped or that $CHCl_3$ acts as a "compatibilizer" for both blocks. To address this issue, we annealed the samples in CH_2Cl_2 vapor for 3 days, followed by slow evaporation and drying *in vacuo*. Figure 2a clearly shows that the Au NPs which were originally distributed throughout P4VP-*b*-PS brushes have now mostly migrated from the P4VP into the PS domain.

As the interaction between brush and NPs depends on the NP shell, one would expect the ligand density of PS on the particles to play an important role in the infiltration. Indeed, Figure 2b shows that NPs with lower PS density ($\Sigma_{PS} = 0.95$ chains nm^{-2}) do not stay inside the PS domain after annealing. Instead, these particles are expelled from the brush completely, ending up at the PS−air interface, where the NPs form clusters reminiscent of the baguette-shaped structures predicted by Kim and O'Shaughnessy.[14] Clearly, the decreased PS density has made the NPs immiscible with both the PS and P4VP domains, reverting to the regime of incompatibility between the NP and the brush.

In contrast to the results shown in Figure 2b, Kim et al.[9] reported that decreasing the PS density on NPs resulted in the NPs accumulating at the PS−P2VP interface. Gupta et al., however, showed that PEO-covered NPs were driven to the air−poly(methyl methacrylate) (PMMA) interface, to increase the entropy of the PMMA chains.[24] In our system, the same effect, combined with the "upward pressure" of the brushes on NPs, could provide a more favorable location for the NPs than the PVP−PS interface.

To confirm the effect of annealing, we measured similar samples as shown in Figure 1 by spectroscopic ellipsometry (SE), before and after annealing. The SE traces were fit to two different models: (i) a layer of Au on top of a pure brush layer and (ii) a mixed layer of Au and brush (Figures S5c, d). We should note that due to the complexity of the optical properties of dispersed Au NPs, it is impossible to completely model the ellipsometric data. However, there is clearly a better fit for the mixed layer model than for the two-layer model before annealing (Figure S5a), indicating NP infiltration. In contrast, after annealing, the fit of the mixed layer has deteriorated significantly (Figure S5b); the sample can no longer be described as fully infiltrated, in agreement with the TEM images shown in Figure 2. Fitting to a two-layer model, mimicking the structure shown in Figure 2, led to degenerate fits due to the complexity of the model.

In summary, we have demonstrated a facile infiltration process, in which gold NPs are assembled into block copolymer brushes. After solvent annealing, the polymer-covered NPs are either sequestered into the corresponding block copolymer domain or expulsed from the brush, depending on the shell density of the NPs. The TEM images clearly showing the distribution of particles are the first examples of direct evidence of the morphology of brush−nanoparticle composites. Further studies will investigate the detailed relationship between NP distribution and brush grafting density and composition.

Acknowledgment. We are grateful to Dr. Madeleine Ramstedt for measuring XPS. Z.L. and R.O. are grateful for EPSRC funding (EP/C015401/1); U.W. was supported by Leverhulme Trust and EPSRC; S.C.W. was supported by the EPA STAR fellowship.

Supporting Information Available: Experimental procedures, additional TEM images, and ellipsometric data are presented. This material is available free of charge via the Internet at http://pubs.acs.org.

References

(1) Balazs, A. C.; Emrick, T.; Russell, T. P. *Science* **2006**, *314*, 1107–1110.
(2) Warren, S. C.; Messina, L. C.; Slaughter, L. S.; Kamperman, M.; Zhou, Q.; Gruner, S. M.; DiSalvo, F. J.; Wiesner, U. *Science* **2008**, *320*, 1748–1752.
(3) Jain, A.; Wiesner, U. *Macromolecules* **2004**, *37*, 5665–5670.
(4) Warren, S. C.; DiSalvo, F. J.; Wiesner, U. *Nat. Mater.* **2007**, *6*, 156–161.
(5) Schultz, A. J.; Hall, C. K.; Genzer, J. *Macromolecules* **2005**, *38*, 3007–3016.
(6) Bockstaller, M. R.; Lapetnikov, Y.; Margel, S.; Thomas, E. L. *J. Am. Chem. Soc.* **2003**, *125*, 5276–5277.
(7) Bockstaller, M. R.; Mickiewicz, R. A.; Thomas, E. L. *Adv. Mater.* **2005**, *17*, 1331–1349.
(8) Chiu, J. J.; Kim, B. J.; Kramer, E. J.; Pine, D. J. *J. Am. Chem. Soc.* **2005**, *127*, 5036–5037.
(9) Kim, B. J.; Bang, J.; Hawker, C. J.; Kramer, E. J. *Macromolecules* **2006**, *39*, 4108–4114.
(10) Thompson, R. B.; Ginzburg, V. V.; Matsen, M. W.; Balazs, A. C. *Science* **2001**, *292*, 2469–2472.
(11) Kunz, M. S.; Shull, K. R.; Kellock, A. J. *J. Colloid Interface Sci.* **1993**, *156*, 240–249.
(12) Snaith, H. J.; Whiting, G. L.; Sun, B.; Greenham, N. C.; Huck, W. T. S.; Friend, R. H. *Nano Lett.* **2005**, *5*, 1653–1657.
(13) Kim, J. U.; O'Shaughnessy, B. *Macromolecules* **2006**, *39*, 413–425.
(14) Kim, J. U.; O'Shaughnessy, B. *Phys. Rev. Lett.* **2002**, *89*, 238301.
(15) Kim, J. U.; Matsen, M. W. *Macromolecules* **2008**, *41*, 246–252.
(16) Azzaroni, O.; Brown, A. A.; Cheng, N.; Wei, A.; Jonas, A. M.; Huck, W. T. S. *J. Mater. Chem.* **2007**, *17*, 3433–3439.
(17) Santer, S.; Rühe, J. *Polymer.* **2004**, *45*, 8279–8297.
(18) Tokareva, I.; Minko, S.; Fendler, J. H.; Hutter, E. *J. Am. Chem. Soc.* **2004**, *126*, 15950–15951.
(19) Bhat, R. R.; Genzer, J. *Appl. Surf. Sci.* **2006**, *252*, 2549–2554.
(20) Husseman, M.; Malmström, E. E.; McNamara, M.; Mate, M.; Mecerreyes, D.; Benoit, D. G.; Hedrick, J. L.; Mansky, P.; Huang, E.; Russell, T. P.; Hawker, C. J. *Macromolecules* **1999**, *32*, 1424–1431.
(21) Matyjaszewski, K.; Woodworth, B. E.; Zhang, X.; Gaynor, S. G.; Metzner, Z. *Macromolecules* **1998**, *31*, 5955–5957.
(22) McCaffrey, J. P. *Ultramicroscopy* **1991**, *38*, 149–157.
(23) Spence, J. C. H.; Zuo, J. M. *Electron Microdiffraction*; Plenum: New York, 1992.
(24) Gupta, S.; Zhang, Q.; Emrick, T.; Balazs, A. C.; Russell, T. P. *Nat. Mater.* **2006**, *5*, 229–233.

JA8090092